

Large Field Background Oriented Schlieren for Visualising Heated Air Projection of Fan Heaters

Mark J Adkin, John Lamb

Dyson Ltd

Tetbury Hill, Malmesbury, Wiltshire, SN16 0RP, UK

mark.adkin@dyson.com; john.lamb@dyson.com

Abstract - The Background Orientated Schlieren (BOS) technique has been applied to a large scale flow field for the development of fan heaters at Dyson. The technique was applied successfully to capture a field-of-view of $2\text{m} \times 1\text{m}$, clearly showing the difference in fan heater projection characteristics. The level of pixel shift was found to be relatively small and there was a presence of artefacts for small interrogation windows. An extension to the BOS technique has been explored, including a novel background designed specifically for its auto-correlation properties. This background explores the properties of a unipolar Maximum Length Sequence (MLS), which is designed to be robust to noise. The new technique was successfully applied to a fan heater and was shown to provide a subjective improvement in artefact reduction. A metric was sought to quantify the merits of this approach to background design.

Keywords: Background oriented schlieren, Fan heater, Visualisation, Heat projection, Maximum length sequence.

1. Introduction

Dyson launched its AM04 fan heater shown in fig. 1(a) in 2011. The fan heater has a race track shaped manifold containing two heater elements in which air is heated before exiting through a thin aperture, forming a jet. A compressor located in the base of the machine will draw the air through a perforated grill. The jet entrains ambient air through the centre and from the sides of the manifold increasing the total volumetric flow rate by a factor of 6. The relatively high velocity of the jet enables the horizontal momentum of the hot air flow to be more prevalent over the effects of buoyancy than conventional fan heaters, giving greater horizontal projection.

Schlieren imaging provides a method of visualising density gradients within a fluid body, allowing the hot and cold regions of the flow to be identified (Settles, 2001). Traditional schlieren methods can capture fine detail, but are usually limited to visualising small flow fields. This restriction is imposed by the prohibitive cost of the collimating mirrors necessary to realise the parallel beams of light over a large field of view.

Recent advances in digital photography and increased computational resources have led to the development of Background Oriented Schlieren (BOS) imaging (Meier, 2002). BOS is highly scalable in terms of the size of the flow field that can be imaged as the acquisition process does not require the use of collimating mirrors. As high resolution digital cameras are now widely available and large backgrounds can be printed relatively cheaply, BOS imaging has become an increasingly accessible tool for large field of view visualisation of hot air flows.

Previously, BOS imaging has been successfully applied to visualise the flow field exiting a HVAC system (Hargather & Settles, 2011). In this study, the field-of-view has been extended to visualise the large scale flow field development from domestic fan heaters. An added study of a background image designed specifically with the post-processing techniques in mind was performed, aimed at improving noise rejection for smaller interrogation window sizes.

2. Background Oriented Schlieren

BOS has traditionally been implemented with a randomly speckled background, digital camera and a computer. Images of the background are taken with and without refractive disturbances (i.e. buoyant jets), which are then post-processed to reveal small distortions.

To post-process these images a cross-correlation method, first set out for PIV (Westerweel, 1997), is employed. The pixel displacement is given by the shift in the cross-correlation peak (lag) between interrogation windows sampled from the reference and measurement images. The 2D correlation operation returns a lag coefficient for the vertical and horizontal directions simultaneously, allowing the density gradients to be resolved in two directions at once. Traditional schlieren resolves the density gradients in only one orientation at a time, since the knife-edge can only enhance contrast in a direction orthogonal to the blade. The BOS image for either the vertical or horizontal deflection is then generated from the correlation lag values returned by scanning the interrogation window over the entire background, allowing visualisation of the hot flow.

The correlation lag value represents the pixel displacement averaged over all pixels in the interrogation window. Features smaller than the interrogation windows are therefore ‘averaged out’ by the correlation operation which acts as a spatial low pass filter. To capture the smallest features, the interrogation window must be made as small as possible. As the interrogation window is made smaller, determining the correlation lag can become increasingly ambiguous, resulting in the introduction of artefacts (noise) in the final BOS image. The ambiguity occurs because the smaller windows are less robust to external noise, causing the amplitude of the correlation peak to be reduced while the sideband energy is increased. External noise can be introduced through several mechanisms including the quality of the optical system, geometrical setup and during post-processing. Selecting the size of the interrogation window is therefore a compromise between the resolving the smallest flow features and the introduction of noise in the final image.

3. Flow Field Visualisation Using a Randomly Generated Background Image

To evaluate how well suited BOS was for capturing the development of the hot air flow field of a fan heater, an experimental investigation of the technique was performed using a randomly generated background.

To capture the relevant flow development of a fan heater a field-of-view of $2\text{m} \times 1\text{m}$ was desired. Setting the test plane equidistant from the camera and the background, a $4\text{m} \times 2\text{m}$ background was required, as shown in fig. 1(b). Initially the background was generated using a quasi-random scalar generator in MATLAB with the values then quantised to either 0 or 1 corresponding to white and black pixels respectively in the final image. The backgrounds needed to be securely mounted on stiff board to stop any deformation.

The total number of pixels was chosen so that a pixel on the background image corresponded to a 2 by 2 pixel grid on the camera sensor. This ratio was chosen because it has been shown to be beneficial in reducing ambiguity in PIV (Raffel, et al., 2007; Vinnichenko, et al., 2012).

The test setup is illustrated in fig. 1(b). The fan heater was placed on a raised plinth at half the distance between the background and the camera. The camera was mounted on a tripod and triggered with a remote. The camera used is a Nikon D3200, which has a 6016×4000 pixel sensor, with a NIKKOR 50mm f/1.4D lens. A combination of ambient lighting and a 300W spot light was used to illuminate the background, allowing a reasonable f-stop, sensitivity and shutter speed of f/8, ISO400 and 1/6 sec respectively.

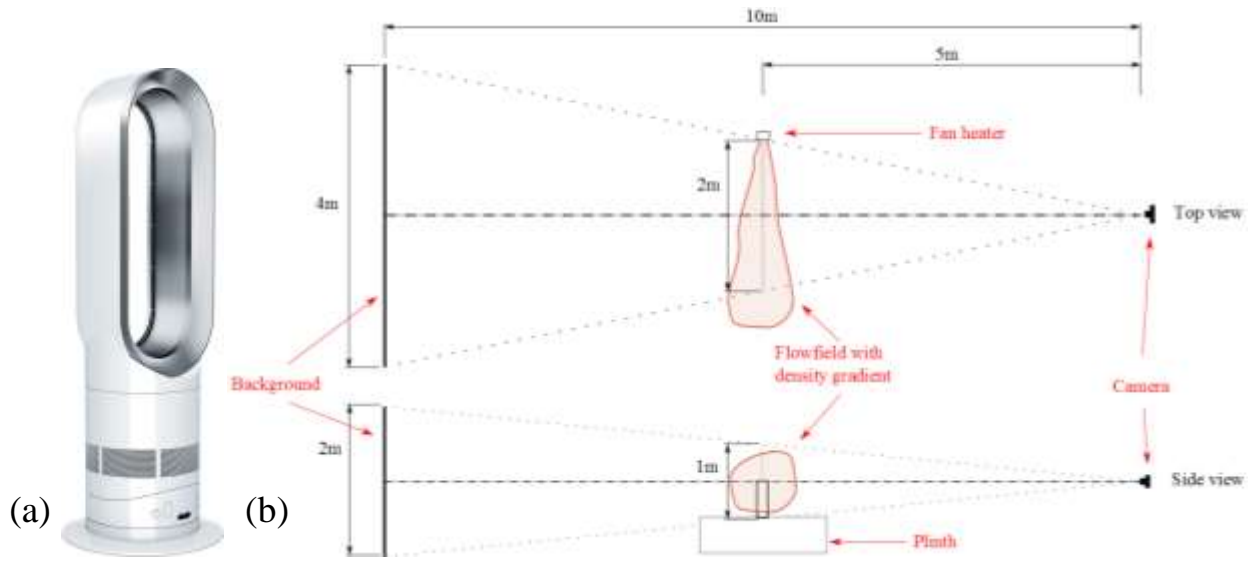


Fig. 1. (a) Dyson AM04 Heater. (b) Setup of large scale BOS test. Flow field containing density gradient is placed equidistant between the camera and the background.

The resultant image of the heated airflow with a field-of-view of $2\text{m} \times 1\text{m}$ can be seen in fig. 2. This image was generated using a 32×32 pixel non overlapping interrogation window. This image demonstrates how the key features of the flow can be successfully visualised. The hot air from the fan heater is projected across the 2m field-of-view, and the jet is clearly increasing in size as it entrains the surrounding air.

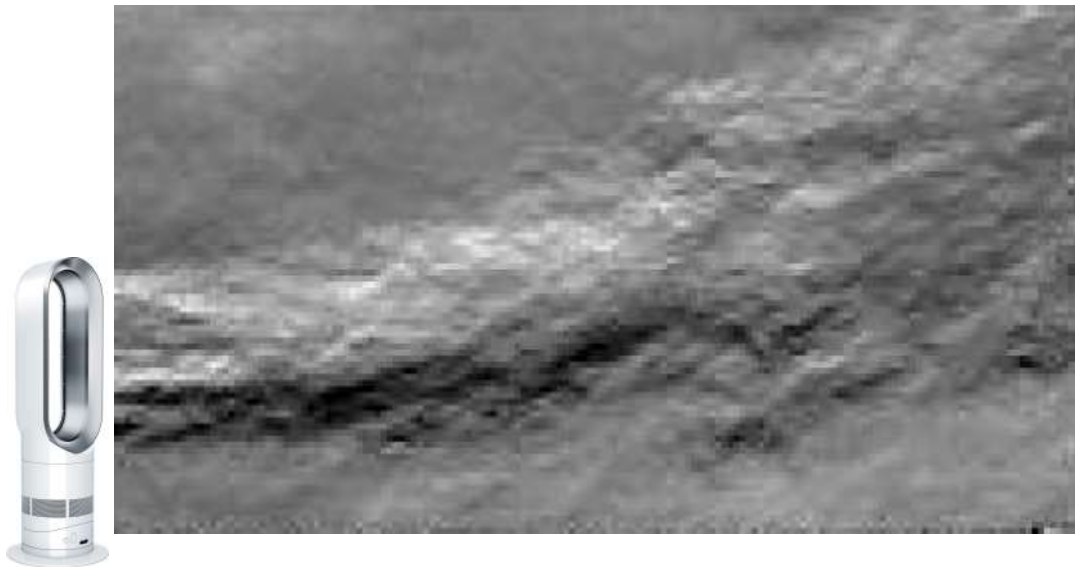


Fig. 2. Resultant vertical deflection image of an AM04 fan heater – showing the projection of hot flow across the $2\text{m} \times 1\text{m}$ field-of-view. Random background with interrogation window size of $32 \times 32\text{px}$.

To assess if the resolution of the resultant image could be improved, a 16×16 pixel interrogation window was used, shown in fig. 3. The higher resolution image reveals finer structure in the flow, but is accompanied by the introduction of artefacts, giving the image a grainy appearance.

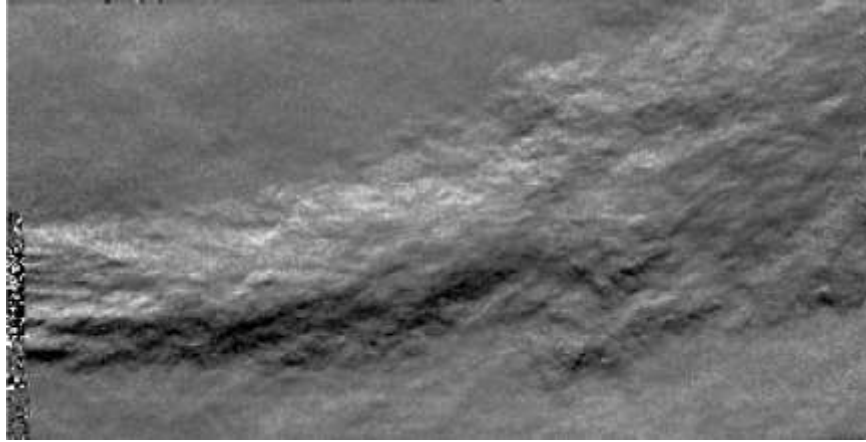


Fig. 3. Resultant vertical deflection image of AM04 UK heater. Random background with interrogation window size of 16×16 px.

The level of these artefacts appears to be of similar size to the deflections that are being captured indicating a low signal to noise ratio. The signal to noise ratio can be improved by increasing the relative pixel deflection on the camera sensor. To achieve this, the distance between the camera and the test plane can be increased, which for a given angular deflection results in larger pixel displacement at the image plane. In this instance, there was insufficient laboratory space to increase the distance between the test and image planes; therefore alternative methods of reducing these artefacts were sought.

4. Flow Field Visualisation Using a MLS Background Image

To enhance BOS, other methods of improving the image quality were investigated. Previously, image deformation techniques, introduced by Huang (Huang, et al., 1993) for PIV post processing have been investigated as a means to improve the resolution with multi-pass images (Scarano, 2002). Others have investigated more general post-processing techniques with regards to algorithm choice (Atcheson, et al., 2009) and background image design for optical accuracy (Vinnichenko, et al., 2012).

The approach taken in this study was to design a background with an ideal autocorrelation function. The premise being that this would result in a background more robust to external noise, reducing the ambiguity and minimising the introduction of artefacts for small interrogation windows.

1D sequences with ideal autocorrelation functions are well known in the signal processing and communications literature (Rife & Vanderkooy, 1989; Schreoder, 1979). A unipolar Maximum Length Sequence (MLS) is a pseudo random train of values alternating between 1 and 0 with length $L = 2^n - 1$, where n is an integer. The normalised autocorrelation function of the unipolar MLS is 1 at zero lag and $(4/(L-3))$ at all other lags. This sequence is very robust to noise, whose influence is spread out over the entire length of the sequence, minimising its effect on the correlation peak and sideband energy.

A mathematical technique, known as the Chinese remainder theorem, can be used to convert these 1D sequences into a 2D image matrix, whilst preserving the ideal autocorrelation and noise rejection properties (D'Antonio, 1998; Angus & D'Antonio, 1999; MacWilliams & Sloane, 1976). The procedure wraps the sequence diagonally into an image matrix ensuring that each element of the sequence appears once. This is possible only if the number of rows P and the number of columns Q are co-prime, such that their only common divisor is 1. There are a limited number of values for P and Q that will accept the MLS sequence, eg. 9×7 , 17×15 and 33×31 . The resultant image for a 17×15 pixel image can be seen in

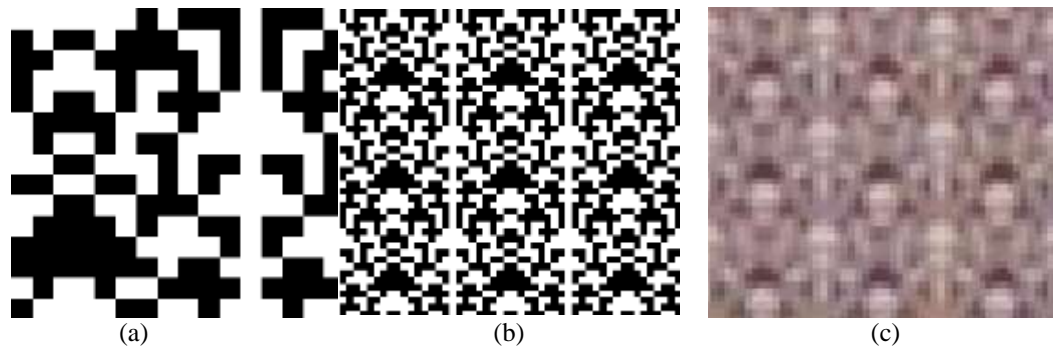


fig. 4(a).

The ideal autocorrelation properties of the MLS image are only preserved if the entire image is contained within the interrogation window. To ensure this is always the case, the interrogation window is chosen to be the same size as the MLS image. As the MLS image is unique, the image must be tiled to interrogate more than one window. A limitation of using a tiled image is that it fixes the size of the interrogation window. The periodic arrangement of the tiles results in a periodic auto-correlation function when window sizes larger than the single tile unit cell are used.

A unipolar MLS sequence of order 8 was chosen with total length $L = 255$ samples. This sequence was wrapped diagonally into a 17×15 image matrix. This was then tiled in a 354×266 grid, giving a 6018×3990 pixel image, with a 1:1 printed pixel to camera pixel representation. The MLS image tile is shown in

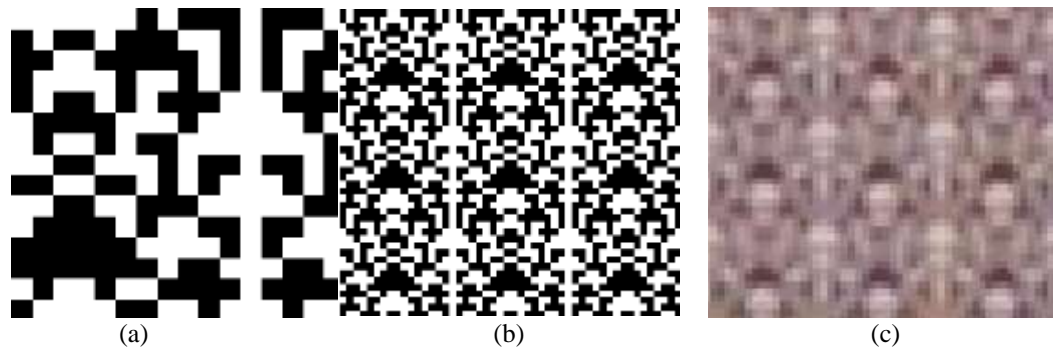


fig. 4 (a), with a small section of repeated tile sequence shown in

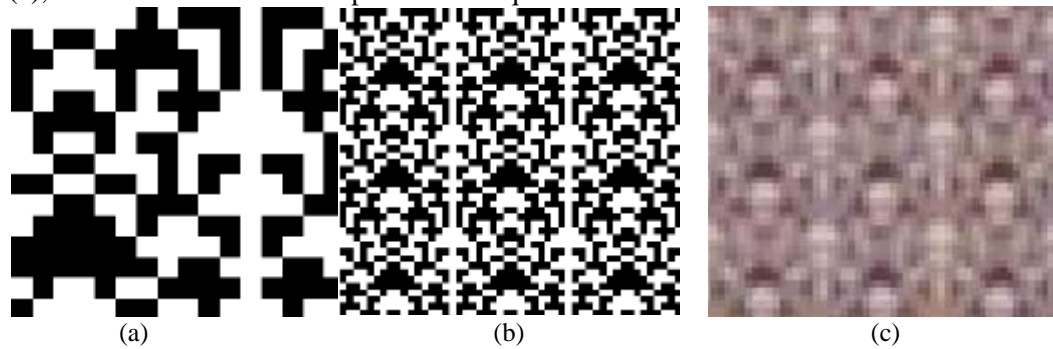


fig. 4 (b). A similarly sized section of the captured image is shown in

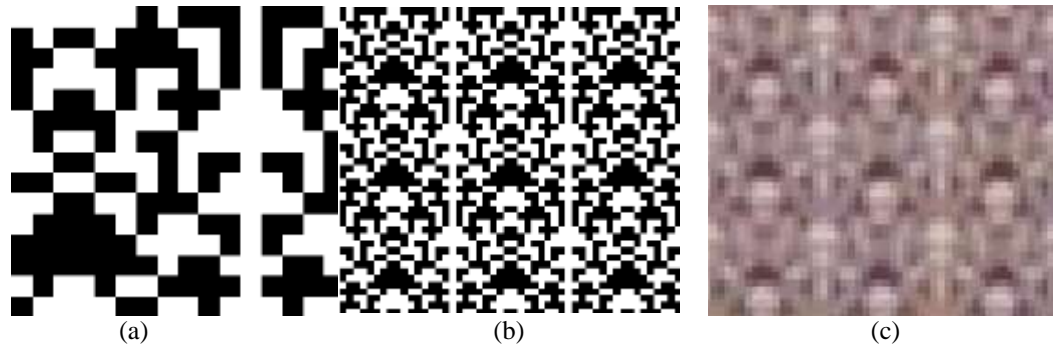


fig. 4 (c). The significant blur in the captured image is due to the limitations of the experimental configuration.

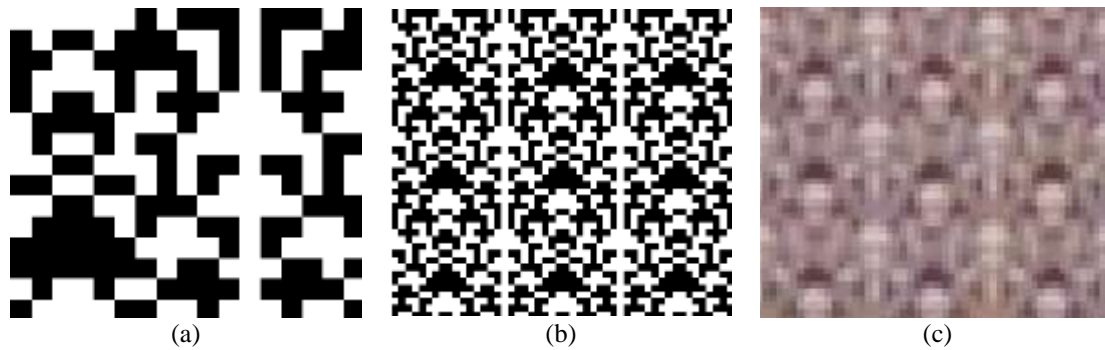


Fig. 4. (a) Maximum Length Sequence (MLS) Tile- 17×15 px. (b) Repeat tile sequence. (c) Captured image of tiles.

The test as described in section 3 was repeated using the MLS tiled BOS background. The practical usage of this background is the same as before apart from the size of the interrogation window used (from 16×16 to 17×15 pixels). Reshaping of the MLS BOS image is required after the post-processing step as the non square interrogation window skews the representation in the resultant image.

Fig. 5(a) and (b) show the resultant BOS images for the random and MLS background respectively. The overall level of noise appears to be similar in both images. The magnified views presented in fig. 5(c) & (d) show the MLS BOS image appears to be slightly smoother with less speckle than the image generated with the random background.

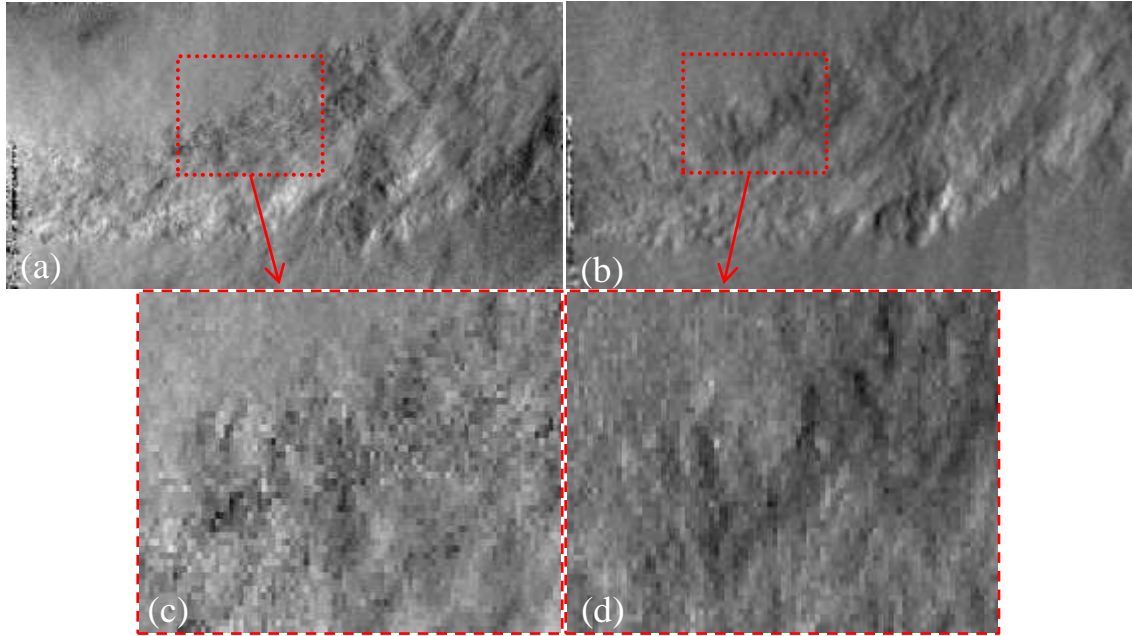


Fig. 5. (a) Horizontal deflection of random background with 16×16 px interrogation windows. (b) Horizontal deflection of MLS tiled background with 17×15 px interrogation windows. (c) and (d) are close-ups of (a) and (b) respectively.

To investigate whether the MLS background was capable of reducing the ambiguity in determining the correlation lag, the cross-correlation function of each interrogation window was normalised and then averaged over the entire image. In fig. 6 (a) and (b) the average cross-correlation functions are presented for the random background and the MLS background respectively. The auto-correlation functions of a random and MLS tile are shown in fig. 6 (c) and (d) respectively for reference.

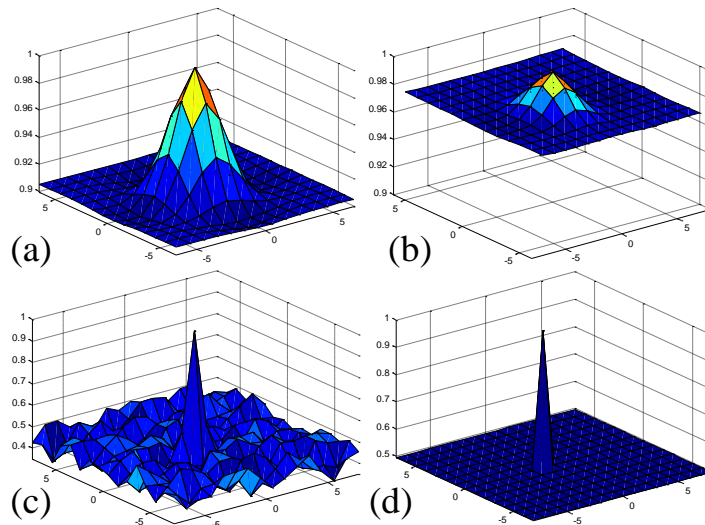


Fig. 6. (a) Average cross-correlation coefficient surface plot for random background image in fig. 3. (b) Average cross-correlation coefficient surface plot for MLS background image in fig. 7(a). (c) Auto-correlation coefficient surface plot for a random background image. (d) Auto-correlation coefficient surface plot demonstrating the ideal autocorrelation function for a MLS background image.

The crest value (ratio of maximum to RMS value) of the MLS average auto-correlation function is 1.028, while the crest value of the random background is 1.097. Qualitatively, this suggests that the MLS background is actually worse at rejecting external noise and warrants further investigation.

5. Application to Fan Heaters

The new MLS background was used to visualize the flow field development of several commercial fan heaters. The technique has been particularly useful for assessing the projection of hot flow, allowing the differences between machines to be clearly highlighted, see fig. 7.

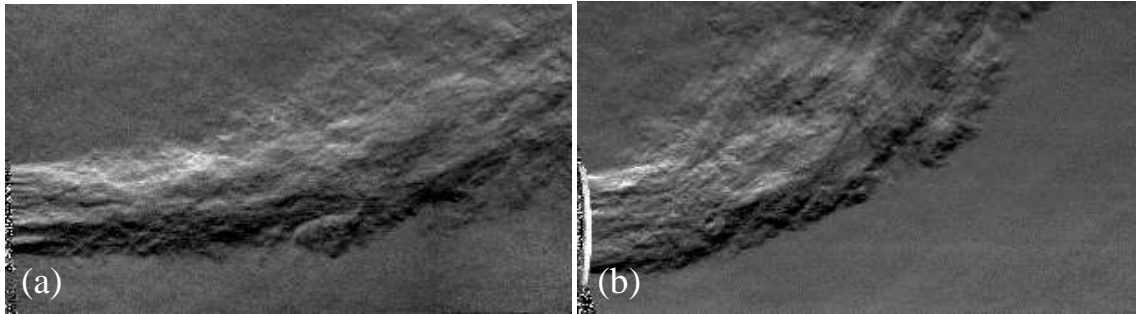


Fig. 7. Resultant vertical deflection image large scale MLS background (a) AM04 UK heater (b) Conventional fan heater.

Fig. 7 clearly reveals that AM04 has significantly higher source momentum, leading to a greater flow projection, whilst the conventional fan heater has more dominant source buoyancy giving a plume like behaviour. This technique provides a low-cost and relatively simple setup for visualising large-scale thermal flows.

6. Conclusion

In this study, large field-of-view ($2\text{m} \times 1\text{m}$) BOS imaging has been successfully demonstrated. With the extended field-of-view, the hot air flow field development of fan heaters can be captured in full. This technique is applicable to a wide range of thermal flows and is particularly appropriate for studying buoyant jets.

The sizes of deflections from the flow field were small and therefore the comparative levels of the artefacts were high for small interrogation windows. To improve BOS image resolution without introducing artefacts, a new scheme of background design was investigated. A background image design approach based on mathematical sequences with ideal autocorrelation functions was developed. Subjectively, the new background appeared to produce smoother BOS images with fewer artefacts. An adequate metric to quantify this subjective improvement has yet to be determined.

Future work will look into extracting quantitative data from these new large scale BOS images, such as fluidic length scales and density/temperature profiles. Such information will be key in insuring future designs give the best possible user comfort.

References

- Angus, J. A. S. & D'Antonio, P., (1999). *Two Dimensional Binary Amplitude Diffusers*.
- Atcheson, B., Heidrich, W. & Ihrke, I., (2009). An evaluation of optical flow algorithms for background oriented schlieren imaging. *Experiments in fluids*, 46(3), pp. 467-476.
- D'Antonio, P., 1998. *Planar binary amplitude diffusor*. USA, Patent No. US5817992 A.
- Hargather, M. J. & Settles, G. S., (2011). *Background-oriented schlieren visualization of heating and ventilation flows: HVAC-BOS*. Daegu.
- Huang, H. T., Fiedler, H. E. & Wang, J. J., (1993). Limitation and improvement of PIV. *Experiments in Fluids*, 15(4-5), pp. 263--273.
- MacWilliams, F. J. & Sloane, N. J. A., (1976). Pseudo-Random Sequences and Arrays. *IEEE*, December, 64(12), pp. 1715-1729.
- Meier, G., (2002). Computerized background-oriented schlieren. *Experiments in Fluids*, pp. 181--187.

- Raffel, M., Wereley, S., Kompenhans, J. & Willert, C., (2007). *Particle Image Velocimetry: A Practical Guide*. 2nd ed. Springer.
- Rife, D. D. & Vanderkooy, J., (1989). Transfer-Function Measurement with Maximum-Length Sequences. *J. Audio. Eng. Soc.*, June, 37(6), pp. 419-44.
- Scarano, F., (2002). Iterative image deformation methods in PIV. *Measurements Science and Technology*, 13(1), pp. R1-R19.
- Schreoder, M. R., (1979). Integrated-impulse method measuring sound decay without using impulses. *J. Acoust. Soc. Am*, Volume 66, pp. 497-500.
- Settles, G. S., (2001). *Schlieren and shadowgraph techniques*. Berlin: Springer-Verlag.
- Settles, G. S., (2010). *Important developments in schlieren and shadowgraph visualization during the last decade*. Daegu, Korea, Int. Symp. on Flow Vis. 2010.
- Settles, G. S., Hackett, E. B., Miller, J. D. & Weinstein, L. M., (1995). *Full-scale schlieren flow visualization*. New York, Flow Visualization VII.
- Vinnichenko, N. A., Uvarov, A. V. & Plaksina, Y. Y., (2012). *Accuracy of Background Oriented Schlieren for different background patterns and means of refraction index reconstruction*. Minsk, Belarus, 15th Int. Symp. Flow Visualization.
- Westerweel, (1997). Fundamentals of digital particle image velocimetry. *Experiments in Fluids*, 29(7), pp. 3-12.